The University of Sydney

Department of Civil Engineering
Sydney NSW 2006
AUSTRALIA

http://www.civil.usyd.edu.au/

Centre for Advanced Structural Engineering

Non-Linear Elastic Non-Uniform Torsion

Research Report No R828

N S Trahair BSc BE MEngSc PhD DEng

June 2003

The University of Sydney

Department of Civil Engineering
Centre for Advanced Structural Engineering
http://www.civil.usyd.edu.au/

Non-Linear Elastic Non-Uniform Torsion

Research Report No R828

N S Trahair BSc BE MEngSc PhD DEng

June 2003

Abstract:

This paper is concerned with large twist rotations of elastic thin-walled open section beams which induce additional longitudinal stresses which exert non-linear "Wagner" stiffening torques.

The non-linear behaviour of a narrow rectangular beam is first analysed and then this is extended to elastic beams of general cross-section. Expressions are derived for the non-linear "Wagner" section constants for narrow rectangular sections, doubly symmetric I-sections, and mono-symmetric equal angle sections.

A general finite element method of analyzing non-linear torsion is described, and used to develop a computer program FENLT. This program can analyse a beam of general cross-section under any combination of concentrated and distributed torques and concentrated bimoments, and which may be prevented from twisting or warping at points along its length. The program is validated by comparison with closed form or numerical solutions for a number of simple examples.

Keywords:

Elasticity, non-linear, non-uniform, open sections, thin-walled, torsion, twist, warping.

Copyright Notice

Department of Civil Engineering, Research Report R828
Non-Linear Elastic Non-Uniform Torsion

N.Trahair@civil.usyd.edu.au

Published by:
Department of Civil Engineering
The University of Sydney
Sydney NSW 2006
AUSTRALIA

June 2003

http://www.civil.usyd.edu.au

INTRODUCTION

The elastic non-uniform torsion of thin-walled open section beams is usually modeled as being linear (Timoshenko and Gere, 1961; Vlasov, 1961; Trahair et al, 2001), but at high angles of twist rotation ϕ, longitudinal stresses induced by the axial shortening of the longitudinal fibres cause significant non-linear stiffening (and strengthening) effects, as indicated in Fig. 1. The basic differential equation for non-linear elastic non-uniform torsion is

$$M_z = GJ\frac{d\phi}{dz} - EI_w\frac{d^3\phi}{dz^3} + \frac{1}{2}EI_n\left(\frac{d\phi}{dz}\right)^3 \quad (1)$$

in which M_z is the torque at a distance z along the torsion member, G and E are the shear and Young's moduli of elasticity, J is the uniform torsion section constant, I_w is the warping section constant, and I_n is a section property that might be described as a non-linear "Wagner" constant. Equation 1 represents the equilibrium between the external torque M_z at z and the internal torsion resistances of the cross-section. These are the linear uniform torque $GJ\,d\phi/dz$, the linear warping torque $-EI_w\,d^3\phi/dz^3$, and the non-linear torque $EI_n(d\phi/dz)^3/2$.

Significant non-linear elastic torsion effects rarely occur in practice because serviceability considerations usually limit the twist rotations to small values at which the non-linear effects are negligible. However, the existence of non-linear torsion effects are important for some aspects of member strength, even though they are not directly incorporated in formulations for member strength.

Firstly, the strengthening effects of non-linear torsion allow torsion members to become fully plastic, as shown in Fig. 2 (Farwell and Galambos, 1969; Pi and Trahair, 1995), and thereby permit the use of plastic methods of strength design for torsion (Trahair et al, 2001). Secondly, non-linear torsion effects also ensure that the elastic post-lateral buckling behaviour of beams is at least imperfection insensitive (Woolcock and Trahair, 1974; Trahair, 1993), as shown in Fig. 3. Thirdly, it is the existence of the stiffening effects of non-linear torsion that justifies the assertion illustrated in Fig. 4 that the lateral buckling strength M_b of a beam bent about its strong axis cannot be less than its weak axis in-plane strength M_{sy} (Trahair, 1997).

There have been a number of previous studies of elastic non-linear torsion (Cullimore, 1949; Woolcock and Trahair, 1974; Pi and Trahair, 1995), but these have largely been limited to doubly symmetric sections. One purpose of this paper is to extend the analysis of non-linear torsion to members of more general cross-section.

The general solution of Equation 1 is not easy because of the non-linear term. A second purpose of this paper is to show how a simple finite element computer program can be developed and used to solve non-linear torsion problems.

Because of the difficulty in solving non-linear torsion problems, an approximate method has been developed and used in the assessment of the lateral buckling strength of angle section beams (Trahair, 2003). A third purpose of this paper is to examine the accuracy of this approximate method.

BASIC BEHAVIOUR

Narrow Rectangular Sections

Fig. 5 shows an initially untwisted narrow rectangular section b x t member of length L after an end-to-end twist rotation of 180°. A longitudinal fibre at a distance a_0 from the axis of twist becomes helical, and rotates $a_0\, d\phi /dz$ as shown in Fig. 6a. Thus a length δz has an apparent axial shortening δw given by

$$-\delta w = \frac{1}{2}\left(a_0 \frac{d\phi}{dz}\right)^2 \delta z \tag{2}$$

as shown in Fig. 6b. The total shortening of the fibre is therefore given by

$$-w = \frac{1}{2} {a_0}^2 \int_0^L \left(\frac{d\phi}{dz}\right)^2 dz \tag{3}$$

However, this shortening requires gross shear straining and warping of the end cross-section to have taken place, as indicated in Fig. 5. If the end of the beam remains plane and unwarped as shown in Fig. 5, then axial strains must be introduced together with the corresponding stresses

$$\sigma_n = \sigma_{n0} - E\frac{dw}{dz} \tag{4}$$

in which σ_{n0} is such that the longitudinal axial force resultant of σ_n is equal to zero. Thus

$$\int_A \sigma_n dA = \sigma_{n0} A + \frac{1}{2} E \left(\frac{d\phi}{dz}\right)^2 \int_A {a_0}^2 dA = 0 \tag{5}$$

in which A is the area of the cross-section, so that

$$\sigma_n = \frac{1}{2} E \left({a_0}^2 - \frac{1}{A}\int_A {a_0}^2 dA \right)\left(\frac{d\phi}{dz}\right)^2 \tag{6}$$

Because of the rotation $a_0\, d\phi /dz$ of the longitudinal fibres, these stresses exert a torque about the axis of twist which is given by

$$M_n = \int_A \sigma_n a_0 \left(\frac{d\phi}{dz}\right) a_0 dA = \frac{1}{2} E I_n \left(\frac{d\phi}{dz}\right)^3 \tag{7}$$

as indicated in Fig. 6c, in which

$$I_n = \int_A {a_0}^4 dA - \frac{1}{A}\left(\int_A {a_0}^2 dA\right)^2 \tag{8}$$

For a narrow rectangular section b x t,

$$I_n = b^5 t \,/\, 180 \tag{9}$$

The non-linear torque M_n is similar to the torque exerted by axial stresses which lead to the torsional buckling of some compression members and which modify the flexural-torsional buckling behaviour of mono-symmetric beams (Trahair, 1993). An early study of these torques was made by Wagner (1936), and so it is appropriate to consider referring to M_n as a non-linear "Wagner torque", and to I_n as a non-linear "Wagner section constant".

General Cross-Sections

The shear centre S(x_0, y_0) of a general cross-section is shown in Fig. 7 together with a general point P(x, y) on the thin-walled section. It is shown in Appendix 3 that the Wagner section constant of a general section is given by

$$I_n = \begin{Bmatrix} [I_{pp} - 4(y_0\beta_x I_x + x_0\beta_y I_y) + 2(x_0^2 - y_0^2)(I_x - I_y) + (x_0^2 + y_0^2)^2 A] \\ -(I_p / A + x_0^2 + y_0^2)^2 A - \beta_x^2 I_x - \beta_y^2 I_y - I_{pw}^2 / I_w \end{Bmatrix} \qquad (10)$$

in which

$$I_x = \int_A y^2 dA \quad , I_y = \int_A x^2 dA \quad , I_w = \int_A \omega^2 dA \qquad (11a)$$

$$I_p = \int_A (x^2 + y^2)\, dA, \quad I_{pp} = \int_A (x^2 + y^2)^2 dA \qquad (11b)$$

$$I_{px} = \int_A y(x^2 + y^2) dA, \quad I_{py} = \int_A x(x^2 + y^2)\, dA, \quad I_{pw} = \int_A \omega(x^2 + y^2)\, dA, \qquad (11c)$$

$$\beta_x = I_{px} / I_x - 2y_0 \quad , \quad \beta_y = I_{py} / I_y - 2x_0 \qquad (11d)$$

and ω is a warping function (Vlasov, 1961).

Doubly Symmetric I-Sections

For doubly symmetric I-sections with flanges b_f x t_f and web b_w x t_w

$$I_n = I_{pp} - I_p{}^2 / A \qquad (12a)$$

$$I_{pp} = \{(6b_f^5 + 20b_f^3 b_w^2 + 30b_f b_w^4)t_f + 3b_w^5 t_w\} / 240 \qquad (12b)$$

$$I_p = \{(2b_f^3 + 6b_f b_w^2)t_f + b_w^3 t_w\} / 12 \qquad (12c)$$

$$A = 2b_f t_f + b_w t_w \qquad (12d)$$

For the special case for which $2b_f = b_w = 2b$ and $t_f = 2t_w = 2t$, these simplify to

$$I_n = 19\ b^5\ t\ /\ 20 \qquad (13)$$

Monosymmetric Equal Angle Sections

For an equal angle b x b x t

$$I_n = b^5\ t\ /\ 90 \qquad (14)$$

FINITE ELEMENT ANALYSIS

A finite element computer program FENLT has been developed for the elastic analysis of non-linear torsion, and is described in Appendix 4. For this program, the member is divided into a number of elements, each of which has a cubic variation of the twist rotation ϕ along its length. The data for each element consists of the values of G, E, J, I_w, I_n, and its length L. Each element may have a uniformly distributed torque per unit length m_z, while concentrated torques M and bimoments B may act at the nodes between elements. Each node may have restraints which prevent twist rotation and/or warping.

A typical graphical output from the program is shown in Fig. 8 for the demonstration example shown in Fig. 9 of an overhanging beam. The upper half of Fig. 8 shows the variations along the member of the normalized twist rotation ϕ/ϕ_{max}, warping ϕ'/ϕ'_{max}, and "twistature" ϕ''/ϕ''_{max}. The lower half shows the variations of the total torque M_z, the uniform torque $GJ\, d\phi/dz$, the warping torque $-EI_w\, d^3\phi/dz^3$, and the non-linear Wagner torque $EI_n (d\phi/dz)^3/2$.

APPLICATIONS

Cantilever

The torque-twist rotation behaviour of a cantilever torsion member of narrow rectangular section 200 mm x 10 mm is shown in Fig. 1. The member has a concentrated torque M acting at the right hand end and is prevented from rotating at the left hand support. The beam properties are G = 80,000 MPa, E = 200,000 MPa , J = 66.667E3 mm^4, I_w = 0 mm^6, I_n = 17.778E9 mm^6, and length L = 1000 mm.

This beam is in uniform torsion under a constant torque $M_z = M$, so that the twist $d\phi/dz$ is constant along the member. In this case, Equation 1 can be solved in closed form as

$$M = GJ\frac{\phi_L}{L} + \frac{1}{2}EI_n\left(\frac{\phi_L}{L}\right)^3 \tag{15}$$

in which ϕ_L is the twist rotation at the free end. This closed form solution is compared in Fig. 1 with the numerical solutions obtained using the computer program FENLT with one element. There is perfect agreement between the two sets of solutions.

Simply Supported Beam

The torque-twist rotation behaviour of a simply supported torsion member of narrow rectangular section is shown in Fig. 10. The member has a uniformly distributed torque per unit length of m_z and is prevented from rotating at both ends. The beam properties are the same as those in the sub-section above.

The torque M_z varies linearly along the beam, so that Equation 1 takes the form of

$$\frac{m_z L}{2}\left(1-\frac{2z}{L}\right)=GJ\frac{d\phi}{dz}+\frac{1}{2}EI_n\left(\frac{d\phi}{dz}\right)^3 \tag{16}$$

Although this cannot be solved in closed form, numerical solutions for the central twist rotation $\phi_{L/2}$ can be obtained by using Gauss quadrature (Burden et al, 1981) in the integration

$$\phi_{L/2}=\int_0^{L/2}\left(\frac{d\phi}{dz}\right)dz \tag{17}$$

in which the values of $d\phi/dz$ at the Gauss points are obtained by solving Equation 16 iteratively. The variation of $\phi_{L/2}$ with m_z obtained in this way is shown in Fig. 10, together with numerical solutions obtained using the computer program FENLT with 8 elements. There is very good agreement between the two sets of solutions.

An approximate closed form solution may be obtained by making the approximations

$$\frac{d\phi}{dz}\approx\frac{4\phi_{L/2}}{L}\left(1-\frac{2z}{L}\right) \tag{18a}$$

$$\left(\frac{d\phi}{dz}\right)^3\approx\frac{32\phi_{L/2}}{L^3}\left(1-\frac{2z}{L}\right) \tag{18b}$$

The first of these approximations is accurate when I_n = 0, while the second provides a corresponding average approximation for $(d\phi/dz)^3$. A similar approximate method was used in Trahair (2003) in a study of the effects of large twist rotations on the lateral buckling strengths of beams with initial twist rotations. When these approximations are substituted into Equation 16, an approximation for the central twist rotation $\phi_{L/2}$ can be obtained by solving

$$\frac{m_z L^2}{2}=4GJ\phi_{L/2}+32\frac{EI_n}{L^2}(\phi_{L/2})^3 \tag{19}$$

It can be seen that the approximate solutions of Equation 19 shown in Fig. 10 underestimate the twist rotations $\phi_{L/2}$.

Slightly more accurate solutions can be obtained by combining the two special solutions of Equation 16 for GJ = 0 and EI_n = 0 as

$$\frac{m_z L^2}{2}=4GJ\phi_{L/2}+\left(\frac{8}{3}\right)^3\frac{EI_n}{L^2}(\phi_{L/2})^3 \tag{20}$$

These overestimate the twist rotations $\phi_{L/2}$. Improved agreement can be obtained for this example by using

$$\frac{m_z L^2}{2}=4GJ\phi_{L/2}+23\frac{EI_n}{L^2}(\phi_{L/2})^3 \tag{21}$$

instead of Equations 19 or 20.

Overhanging Beam

The overhanging I-section beam shown in Fig. 9 is used as a demonstration of the output of the computer program FENLT. This 4 m long beam has a bimoment B = 10 kNm^2 acting at a distance of 1 m from the left hand end, a concentrated torque of M = 20 kNm at a distance of 2 m, and a uniformly distributed torque per unit length of m_z = -20 kNm/m acting from 3 m to 4 m. The beam is prevented from rotating and warping at the left hand end, is prevented from rotating at a distance of 3 m and is prevented from warping at the right hand end. The manual linear analysis of this redundant beam is made very difficult by the different types of actions, the two different types of resistance (uniform and warping torsion), and the different types of boundary conditions, while the manual non-linear analysis is virtually impossible because of the complicating influence of the non-linear Wagner torque.

However, the computer program FENLT can easily allow for all these effects. Its solution for the variation of the twist rotation is shown in the upper half of Fig. 8, which demonstrates the boundary conditions of $\phi = \phi' = 0$ at $z = 0$, $\phi = 0$ at $z = 3$ m, and $\phi' = 0$ at $z = 4$ m. The variation of the total torque shown by the solid line in the lower half of Fig. 8 indicates that the reaction torques are comparatively small. The warping torque has a maximum value at the point where the bimoment is applied. Because the total torque is small at this point, the warping torque is largely balanced by the uniform and non-linear torques, which are also maximum at this point. The total torque changes suddenly at the point where the applied torque acts, and this sudden change produces a corresponding sudden change in the warping torque at this point. Similar but smaller sudden changes occur at the reaction point at $z = 3$ m.

CONCLUSIONS

This paper is concerned with large twist rotations of elastic thin-walled open section beams. Large twist rotations induce additional longitudinal stresses which exert non-linear "Wagner" stiffening torques which are proportional to the cube of the twist per unit length.

It is argued that even though the twist rotations of practical beams are invariably so small that the non-linear torques may be ignored, nevertheless, large twist rotation effects allow plastic methods of torsion design to be used, demonstrate that the post-buckling behaviour of a laterally unsupported beam is not imperfection sensitive, and ensure that the lateral buckling strength of a beam bent about its strong axis is never less than its weak axis in-plane strength. Thus theoretical and numerical research into these types of problem require the ability to carry out the analysis of non-linear torsion.

The non-linear behaviour of an elastic narrow rectangular beam is first analysed and then this is extended to elastic beams of general cross-section. Expressions are derived for the non-linear "Wagner" section constants for narrow rectangular sections, doubly symmetric I-sections, and mono-symmetric equal angle sections.

The manual analysis of non-linear torsion is found to be difficult to carry out, except in a few simple cases. A general finite element method of analyzing non-linear torsion is described, and used to develop a computer program FENLT. This program can analyse a beam of general cross-section under any combination of concentrated and distributed torques and concentrated bimoments, and which may be prevented from twisting or warping at points along its length.

The computer program is validated by comparison with closed form or numerical solutions for a number of simple examples. It is then used to assess and improve the accuracy of an approximate method of analysis.

Appendix 1 – References

Burden, RL, Faires, JD, and Reynolds, AC (1981), *Numerical Analysis*, 2nd edition, PWS Publishers, Boston, Massachusetts.

Cullimore, MSG (1949), "The shortening effect – a non linear feature of pure torsion", *Engineering Structures*, Butterworths Scientific Publication, London.

Farwell, CR and Galambos, TV (1969), "Non-uniform torsion of steel beams in inelastic range", *Journal of the Structural Division*, ASCE, **95** (ST12), 2813-29.

Mathworks Inc (1995), *Student Edition of MATLAB*, Prentice Hall, Englewood Cliffs, NJ.

Pi, YL and Trahair, NS (1995), "Inelastic torsion of steel I-beams", *Journal of Structural Engineering*, ASCE, **121** (4), 609-20.

Timoshenko, SP and Gere, JM (1961), *Theory of Elastic Stability*, 2nd edition, McGraw-Hill, New York.

Trahair, NS (1993), *Flexural-Torsional Buckling of Structure*s, E & FN Spon, London.

Trahair, NS (1997), "Multiple design curves for beam lateral buckling", *Proceedings*, International Colloquium on Stability and Ductility of Steel Structures, Nagoya, 33-44.

Trahair, NS (2003), "Lateral buckling strengths of steel angle section beams", *Journal of Structural Engineering*, ASCE, **129** (6), in press.

Trahair, NS and Bild, S (1990), "Elastic biaxial bending and torsion of thin-walled members", *Thin-Walled Structures*, **9**, 269-307.

Trahair, NS, Bradford, MA, and Nethercot, DA (2001), *The Behaviour and Design of Steel Structures to BS5950*, 3rd edition, Spon Press, London.

Vlasov, VZ (1961), *Thin-Walled Elastic Beams*, 2nd edition, Israel Program for Scientific Translation, Jerusalem.

Wagner, H (1936), "Verdrehung und knickung von offenen profilen (Torsion and buckling of open sections)", *NACA Technical Memorandum*, No. 807.

Woolcock, ST and Trahair, NS (1974), "Post-buckling behavior of determinate beams", *Journal of the Engineering Mechanics Division*, ASCE, **100** (EM2), 151-71.

Appendix 2 – Notation

a_0	distance to shear centre
A	area of section
b	length of rectangular element
b_f, b_w	flange width and web depth
B	bimoment
B_0	correction bimoment
$[B_L]$, $[B_Q]$	matrices for linear and quadratic strains
$[CI]$	matrix for nodal deformations
$[D]$	tangent modulus constitutive matrix
$\{e\}$	vector of equilibrium equation errors
E	Young's modulus of elasticity
$\{F_E\}$	vector of external applied actions
$\{F_I\}$	vector of equivalent internal resistances
G	shear modulus of elasticity
I_n	non-linear Wagner section constant
I_p, I_{pp}, I_{pw}	section properties
I_w	warping section constant
I_x, I_y	second moments of area
J	torsion section constant
$[K_T]$	tangent stiffness matrix
L	length of member or element
m_z	uniformly distributed torque per unit length
M	concentrated torque
M_b	lateral buckling moment capacity
M_e	elastic lateral buckling moment
M_n	non-linear Wagner torque
M_{sx}, M_{sy}	section moment capacities
M_{x0}, M_{y0}	correction moments
M_z	torque at z
$[M_\sigma]$	geometric matrix
N_0	correction axial force
s	distance around thin wall
t	wall thickness
t_f, t_w	flange and web thicknesses
w	deflection in the z direction
x, y	principal centroidal axes
x_0, y_0	shear centre coordinates
z	longitudinal axis through centroid
$\{Z\}$	vector of powers of z/L
β_x, β_y	section properties
$\{\delta_\phi\}$	vector of nodal deformations
$\{\Delta\delta_\phi\}$	vector of nodal deformation increments
ρ_0	perpendicular distance to shear centre
$\{\sigma\}$	generalized stress resultants
σ_n	longitudinal stress
σ_{n0}	correction stress
ϕ	twist rotation

Appendix 3 – General Cross-Sections

The shear centre S(x_0, y_0) of a general cross-section is shown in Fig. 7 together with a general point P(x, y) on the thin-walled section. The principal centroidal x, y axes of the section are defined by

$$\int_A x\,dA = \int_A y\,dA = \int_A xy\,dA = 0 \tag{22}$$

and the coordinates of the shear centre x_0, y_0 by

$$\int_A \omega\,dA = \int_A x\omega\,dA = \int_A y\omega\,dA = 0 \tag{23}$$

in which ω is a warping function (Vlasov, 1961) defined by

$$\omega = \frac{1}{A}\int_A \left\{\int_0^s \rho_0 ds\right\} t ds - \int_0^s \rho_0 ds \tag{24}$$

in which s is the distance around the thin-walled section, t is the wall thickness, and ρ_0 is the perpendicular distance from the shear centre S to the tangent to the wall at P, as shown in Fig. 7.

The following cross-section properties are defined

$$I_x = \int_A y^2 dA \quad , \quad I_y = \int_A x^2 dA \quad , \quad I_w = \int_A \omega^2 dA \tag{25a}$$

$$I_p = \int_A (x^2 + y^2)\,dA, \quad I_{pp} = \int_A (x^2 + y^2)^2\,dA \tag{25b}$$

$$I_{px} = \int_A y(x^2 + y^2)\,dA, \quad I_{py} = \int_A x(x^2 + y^2)\,dA, \quad I_{pw} = \int_A \omega(x^2 + y^2)\,dA, \tag{25c}$$

The distance a_0 from the point P to the shear centre S is given by

$$a_0 = \sqrt{\{(x - x_0)^2 + (y - y_0)^2\}} \tag{26}$$

During twisting, a longitudinal fibre through the point P and at a distance a_0 from the axis of twist through the shear centre S becomes helical, and rotates $a_0\,d\phi / dz$, as shown for example in Fig. 6a. Thus a length δz has an apparent axial shortening $-\delta w$ given by

$$-\delta w = \frac{1}{2}\left(a_0 \frac{d\phi}{dz}\right)^2 \delta z \tag{27}$$

as shown in Fig. 6b. However, this shortening requires gross shear straining to have taken place, as indicated by the example in Fig. 5. If the end of the beam remains plane as shown in the example of Fig. 5, then axial strains must be introduced together with the corresponding stresses. The total axial stresses can be expressed as

$$\sigma_n = -E\frac{dw}{dz} + \frac{N_0}{A} + \frac{M_{x0}y}{I_x} - \frac{M_{y0}x}{I_y} + \frac{B_0\omega}{I_\omega} \tag{28}$$

in which N_0, M_{x0}, M_{y0}, and B_0 are correction actions.

These actions ensure that the variation of the total axial stresses around the cross-section is such that the axial force, major and minor axis moment, and bimoment stress resultants are zero, which reflect the fact that the member is in pure torsion. These stress resultant conditions can be expressed as

$$\int_A \sigma_n dA = \int_A \sigma_n y dA = \int_A \sigma_n x dA = \int_A \sigma_n \omega dA = 0 \tag{29}$$

which enables the total axial stress to be found as

$$\sigma_n = \frac{1}{2} E(\phi')^2 \left\{ a_0^2 - \left(\frac{I_x + I_y}{A} + x_0^2 + y_0^2 \right) - y \left(\frac{I_{px}}{I_x} - 2y_0 \right) - x \left(\frac{I_{py}}{I_y} - 2x_0 \right) - \omega \frac{I_{pw}}{I_w} \right\} \tag{30}$$

Because of the rotation $a_0\, d\phi/dz$ of the longitudinal fibre through P, this stress exerts a torque about the axis of twist through S, as indicated in Fig. 6c. The resultant of this and all similar stresses is given by

$$M_n = \int_A \sigma_n a_0 \left(\frac{d\phi}{dz} \right) a_0 dA = \frac{1}{2} E I_n \left(\frac{d\phi}{dz} \right)^3 \tag{31}$$

in which

$$I_n = \begin{Bmatrix} [I_{pp} - 4(y_0 \beta_x I_x + x_0 \beta_y I_y) + 2(x_0^2 - y_0^2)(I_x - I_y) + (x_0^2 + y_0^2)^2 A] \\ -(I_p / A + x_0^2 + y_0^2)^2 A - \beta_x^2 I_x - \beta_y^2 I_y - I_{pw}^2 / I_w \end{Bmatrix} \tag{32}$$

in which

$$\beta_x = I_{px} / I_x - 2y_0 \quad , \quad \beta_y = I_{py} / I_y - 2x_0 \tag{33}$$

These expressions simplify for the case of doubly symmetric sections for which 0 = x_0 = y_0 = I_{pw}, so that

$$I_n = I_{pp} - I_p^2 / A \tag{34}$$

Appendix 4 – Finite Element Analysis

A finite element computer program FENLT has been developed for the analysis of non-linear non-uniform torsion. For this, the member length is divided into a number of elements. The typical element used has a cubic twist rotation field defined by (Trahair, 1993)

$$\phi = \{Z\}^T [CI]\ \{\delta_\phi\} \tag{35}$$

in which

$$\{Z\}^T = \{1\ \ z/L\ \ (z/L)^2\ \ (z/L)^3\} \tag{36}$$

$$[CI] = \begin{bmatrix} 1 & 0 & 0 & 0 \\ 0 & 0 & L & 0 \\ -3 & 3 & -2L & -L \\ 2 & -2 & L & L \end{bmatrix} \tag{37}$$

$$\{\delta_\phi\} = \{\phi_1\ \ \phi_2\ \ \phi_1'\ \ \phi_2'\}^T \tag{38}$$

in which z is the distance along the element, L is the length of the element, $' \equiv d/dz$, ϕ_1 and ϕ_2 are the values of ϕ at the element ends, and ϕ_1' and ϕ_2' are the values of ϕ' at the element ends.

Trahair and Bild (1990) have described the basis of a finite element computer program for analyzing the non-linear behaviour of thin-walled open sections. They included non-linearities associated with member instability, but ignored non-linear terms such as the non-linear Wagner torque $EI_n (d\phi/dz)^3 / 2$ considered in this paper. Nevertheless, their formulations may be adapted for the non-linear torsion problems of this paper, in the form of equilibrium relationships

$$\{F_E\} = \{F_I\} \tag{39}$$

between the external actions $\{F_E\}$ and the equivalent internal resistances

$$\{F_I\} = \int_0^L [N_\sigma]^T [B_L + 2B_Q]^T \{\sigma\}\, dz \tag{40}$$

and the tangent stiffness

$$[K_T] = \int_0^L [N_\sigma]^T ([B_L + 2B_Q]^T [D][B_L + 2B_Q] + [M_\sigma])[N_\sigma]\, dz \tag{41}$$

In these equations, the external actions $\{F_E\}$ are the nodal torques (consisting of the applied concentrated torques M and the equivalents $m_z L/2$ of the distributed torques per unit length m_z) and the nodal bimoments B, and

$$[N_\sigma] = \begin{bmatrix} \{Z'\}^T \\ \{Z''\}^T \end{bmatrix} [CI] \tag{42}$$

$$[B_L]^T = \begin{bmatrix} 0 & 0 & -1 \\ -1 & 0 & 0 \end{bmatrix}, \qquad [B_Q]^T = \begin{bmatrix} 0 & \phi'/2 & 0 \\ 0 & 0 & 0 \end{bmatrix} \tag{43}$$

$$\{\sigma\}^T = \{-EI_w\phi''\ \ \ EI_n(\phi')^2/2\ \ \ -GJ\phi'\} \tag{44}$$

$$[D] = \begin{bmatrix} EI_w & 0 & 0 \\ 0 & EI_n & 0 \\ 0 & 0 & GJ \end{bmatrix} \tag{45}$$

$$[M_\sigma] = \begin{bmatrix} EI_n(\phi')^2/2 & 0 \\ 0 & 0 \end{bmatrix} \tag{46}$$

In general, the equilibrium equations (39) will not be satisfied, but will lead to a set of errors

$$\{e\} = \{F_E\} - \{F_I\} \tag{47}$$

which may be reduced by introducing a set of deformation changes $\{\Delta\delta_\phi\}$ which satisfy

$$[K_T]\ \{\Delta\delta_\phi\} = \{e\} \tag{48}$$

These changes may be made iteratively until the errors $\{e\}$ are sufficiently small.

Those integrations in Equations 40 and 41 which are associated with the linear terms are made in closed form in the program FENLT. However, it is more convenient for the integrations associated with the non-linear Wagner torque to use Gaussian quadrature (Burden et al, 1981), for which 3 Gauss points per element are usually sufficiently accurate.

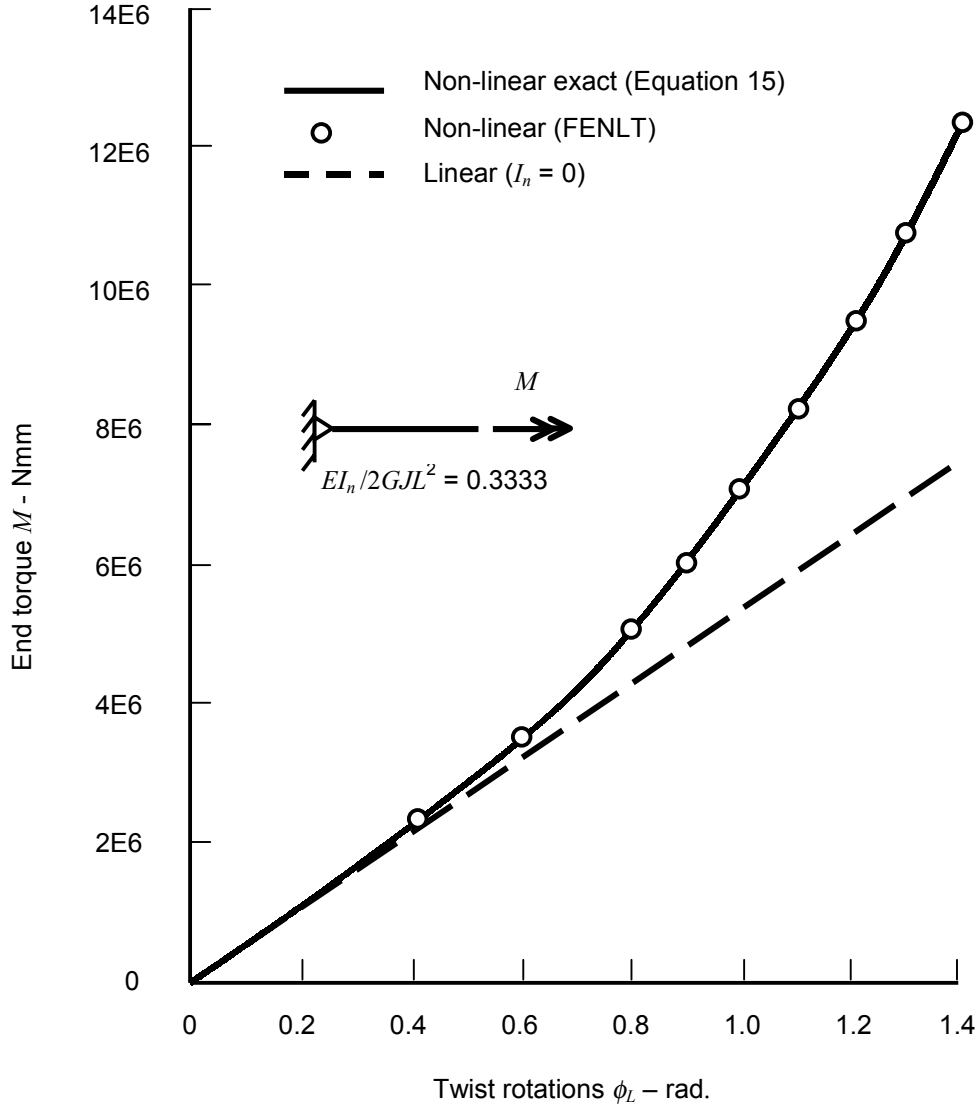

Fig. 1. Large Elastic Twist Rotations of a Cantilever

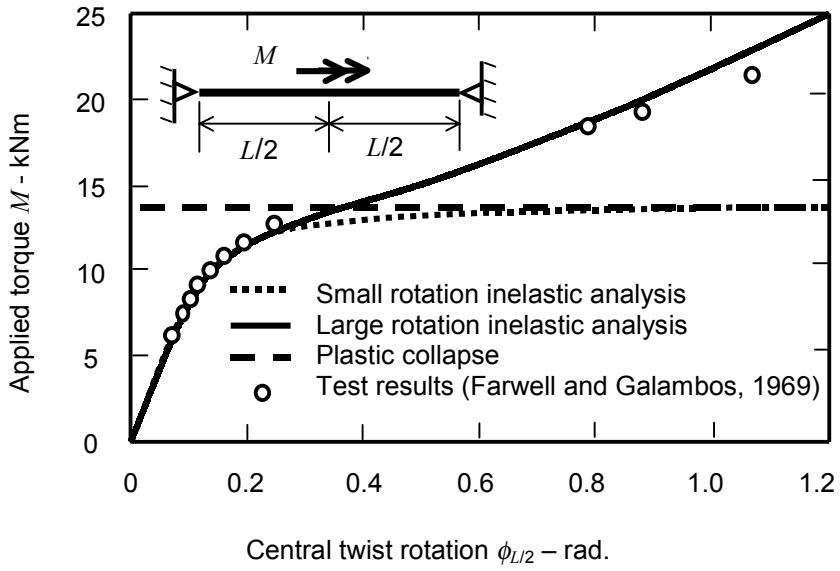

Fig. 2. Large Inelastic Twist Rotations of a Beam

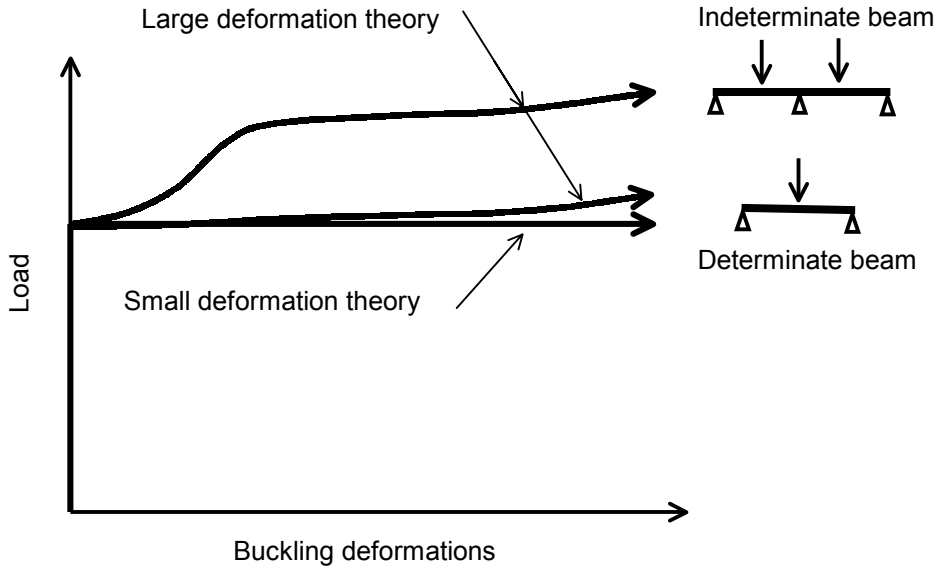

Fig. 3. Post-Buckling Behaviour of Elastic Beams

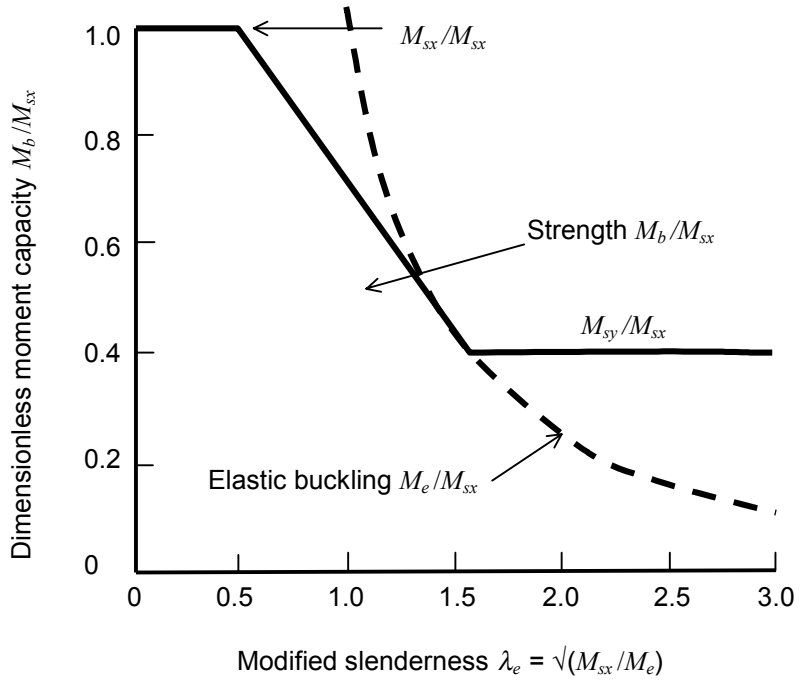

Fig.4. Lateral Buckling Strengths of Steel Beams

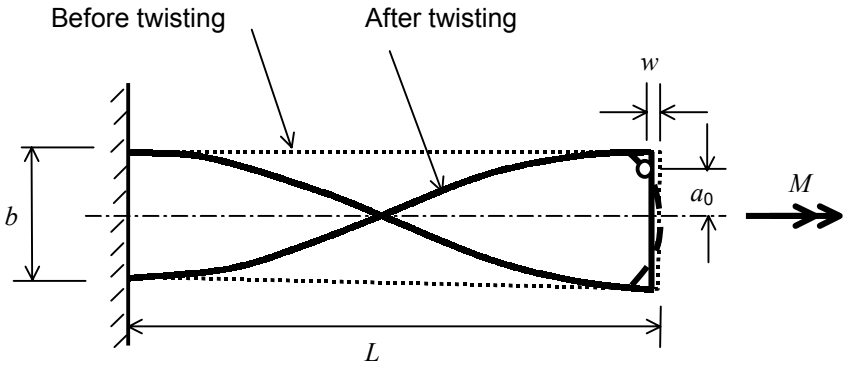

Fig. 5. Large Twist Rotations of a Narrow Rectangular Section

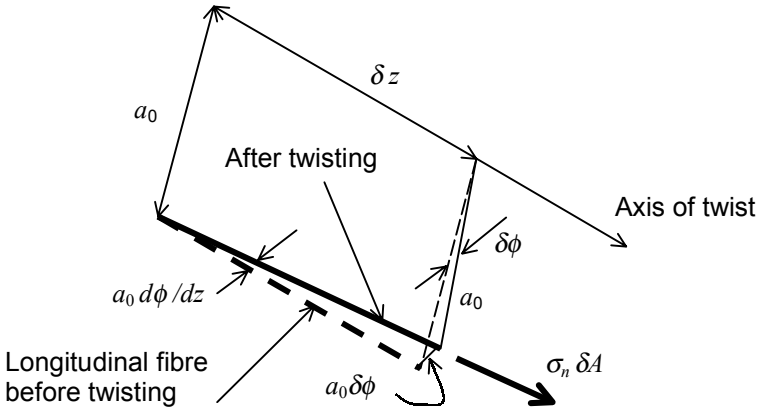

(a) Rotations during twisting

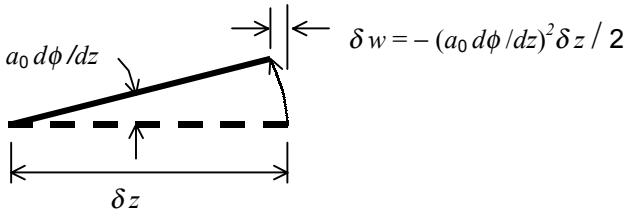

(b) Apparent shortening

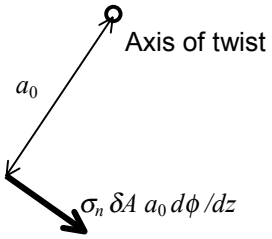

(c) Torque component

Fig. 6. Rotations, Shortening, and Torque Component

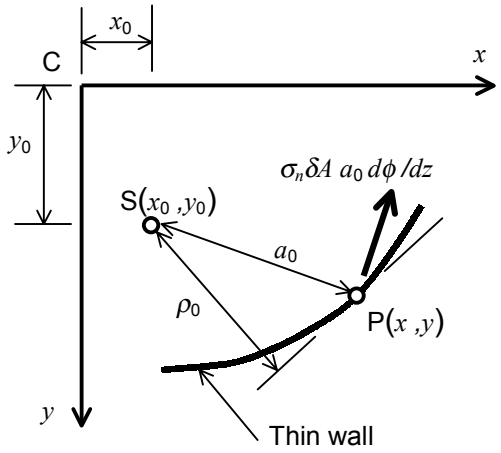

Fig. 7. General Cross-Section

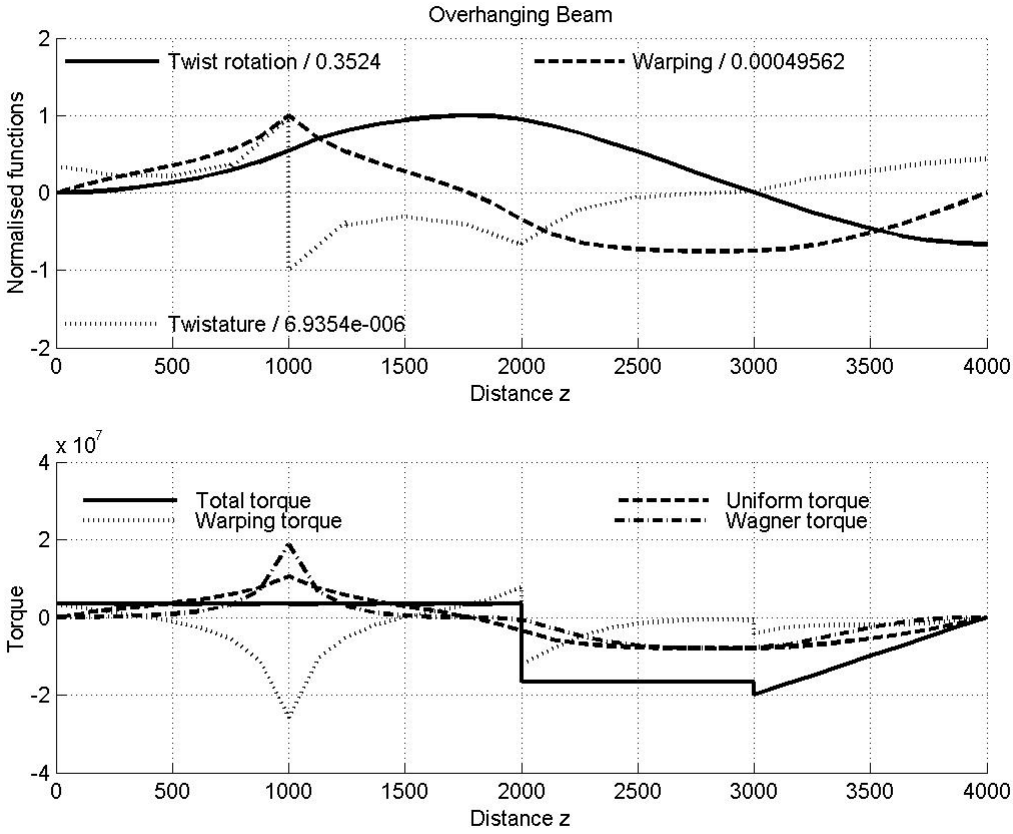

Fig. 8. Graphical Output from FENLT

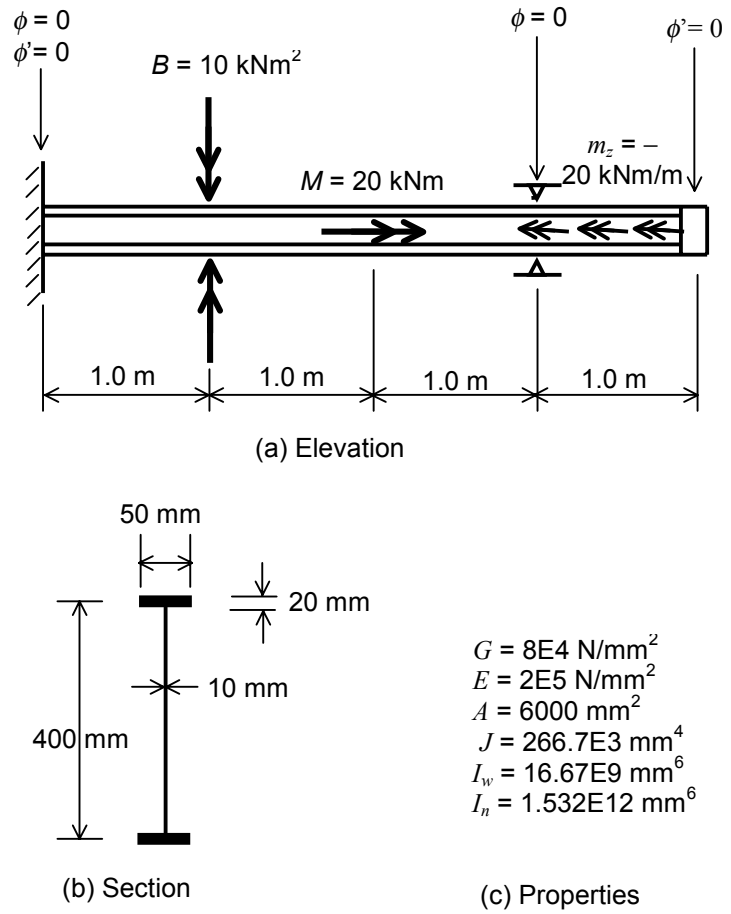

Fig. 9. Demonstration Example – Overhanging Beam

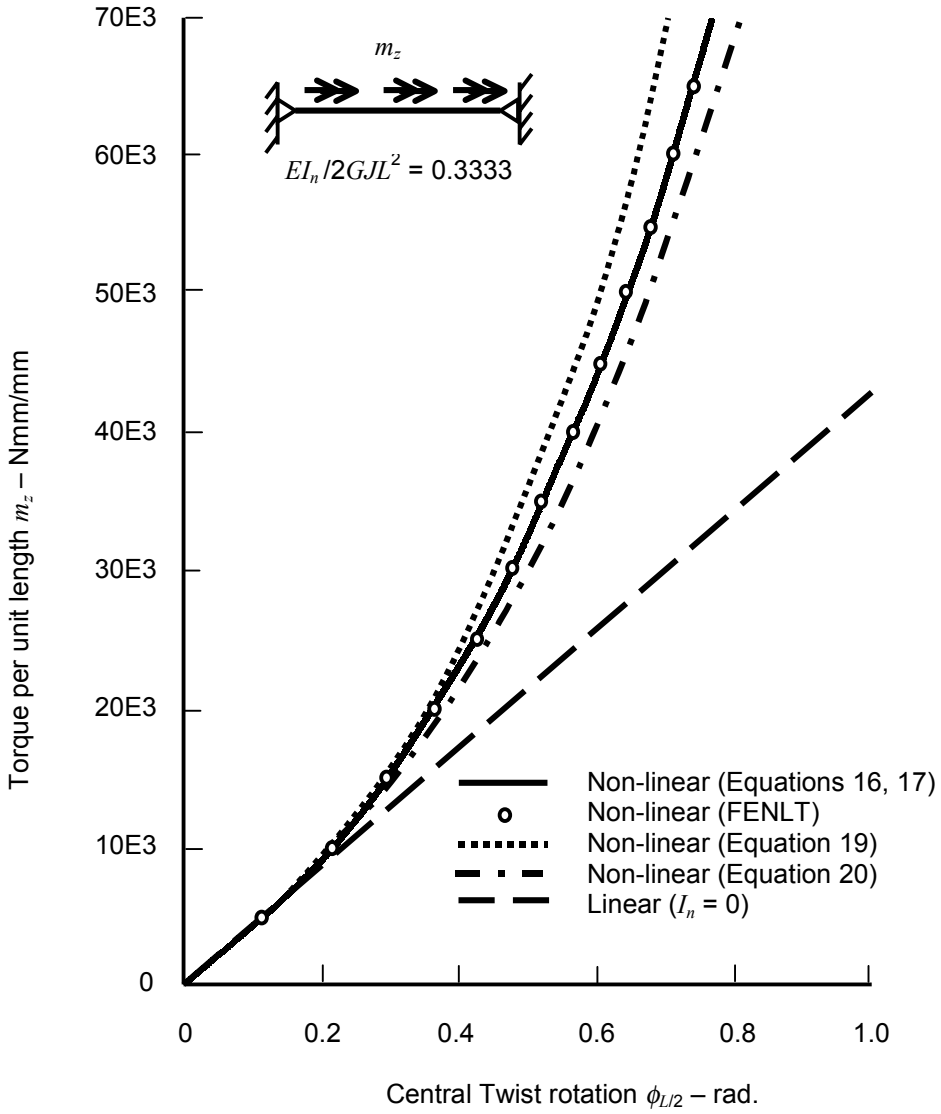

Fig. 10. Large Elastic Twist Rotations of a Beam